SUBJECT: SOI – Geophysical Assistance April 21, 2010

TO: Craig R. Derickson File Code: 330-7
State Conservationist
NRCS, Harrisburg, Pennsylvania

Dr. Henry Lin
Assistant Professor of Hydropedology/Soil Hydrology
Crop & Soil Sciences Department
415 Agricultural Sciences and Industries Building
Pennsylvania State University
University Park, PA 16802

Purpose:
At the request of the Dr. Henry Lin, Associate Professor of Hydropedology/ Soil Hydrology at Pennsylvania State University, geophysical field assistance was provided by the National Soil Survey Center to the Department of Crop and Soil Sciences. Geophysical investigations were conducted within the Shale Hills *Critical Zone Observatory* (CZO) in Huntington County. The main purpose of this assistance was to use ground-penetrating radar (GPR) to characterize the movement of water through soils and across landscape components in a small, steeply-sloping, forested watershed that has developed over highly folded and fractured shale parent rock.

Participants:
Doug Baldwin, Graduate Student, Department of Crop & Soil Sciences, PSU, University Park, PA
Jim Doolittle, Research Soil Scientist, USDA-NRCS-NSSC, Newtown Square, PA
Henry Lin, Associate Professor of Hydropedology/Soil Hydrology, Department of Crop & Soil Sciences, PSU, University Park, PA
Jun Zhang, PhD Student, Department of Crop & Soil Sciences, PSU, University Park, PA

Activities:
Field activities were completed on 13 April 2010.

Summary:
1. Detailed, ground-penetrating radar (GPR) surveys were conducted over three grid sites located in areas of Rushtown and Weikert soils.

2. Copies of the radar records that were collected over the grid sites have been turned-over to the principal investigator, Jun Zhang, for analysis. As part of his research project, Jun is responsible for the analysis of the collected two-dimensional (2D) radar records and the construction and interpretation of three-dimensional (3D) pseudo-images. Data collected during this investigation will add to Jun's research on the infiltration of water in soils underlain by shale parent rock.

3. The synergy of GPR and global positioning systems (GPS) were explored in the Shale Hills Watershed area. These studies are aimed at developing new, cutting-edge technologies to investigate water movement in soils and across landscapes at different spatio-temporal scales.

/s/ Jonathan W. Hempel

JONATHAN W. HEMPEL
Director

National Soil Survey Center cc: See attached list

cc:
Steve Carpenter, MLRA Office Leader, USDA-NRCS, Morgantown, WV
Jim Doolittle, Research Soil Scientist, USDA-NRCS-NSSC, Newtown Square, PA
Michael Golden, Director of Soils Survey Division, USDA-NRCS, Washington, DC
Wes Tuttle, Soil Scientist (Geophysical), USDA-NRCS-NSSC, Wilkesboro, NC
Larry W. West, National Leader, Soil Survey Research & Laboratory, NSSC, MS 41, NRCS, Lincoln, NE
Edgar White, State Soil Scientist, USDA-NRCS, Harrisburg, PA
Mike Wilson, Research Soil Scientist & Liaison for MO13, Soil Survey Research & Laboratory Staff, MS 41, USDA-NRCS-NSSC, Lincoln, NE

Technical Report on Geophysical Investigations conducted at the Shale Hills *Critical Zone Observatory* (CZO) in Huntington County on 13 April 2010.

James A. Doolittle

This study uses cutting-edge geophysical technologies to better understand and characterize how soil "architecture" and distributions on landscapes exert controls over hydrologic processes across spatio-temporal scales (Lin, 2010).

Equipment:
The radar unit is the TerraSIRch Subsurface Interface Radar (SIR) System-3000 (here after referred to as the SIR-3000), manufactured by Geophysical Survey Systems, Inc. (GSSI; Salem, NH).[1] The SIR-3000 consists of a digital control unit (DC-3000) with keypad, SVGA video screen, and connector panel. A 10.8-volt lithium-ion rechargeable battery powers the system. The SIR-3000 weighs about 4.1 kg (9 lbs) and is backpack portable. With an antenna, the SIR-3000 requires two people to operate. Jol (2009) and Daniels (2004) discuss the use and operation of GPR. The 400 and 900 MHz antennas were used in this investigation. The 900 MHz antenna malfunctioned and needs to be returned to GSSI for repairs.

The RADAN for Windows (version 6.6) software program (here after referred to as RADAN; developed by GSSI) was used to process the radar records shown in this report.[1] Processing included: header editing, setting the initial pulse to time zero, color table and transformation selection, range gain adjustments, signal stacking, migration, and high-pass filtration (refer to Jol (2009) and Daniels (2004) for discussions of these techniques).

Using the *Interactive 3D Module* of the RADAN, depths to bedrock were automatically and reasonably accurately picked, and outputted to a worksheet (X, Y, Z format; including latitude, longitude, depths to interface or layer, and other useful data). The Super 3D QuickDraw of RADAN was used to construct 3D pseudo-images of the radar records collected at the grid sites.

Recent technical developments allow the integration of GPR and GPS data. The SIR-3000 provides a setup for the use of a GPS receiver with a serial data recorder (SDR). A Pathfinder ProXT GPS receiver with Hurricane antenna (Trimble, Sunnyvale, CA) was used to georeferenced GPR data.[1] With this setup, each scan of the radar can be georeferenced (position/time matched). Following data collection, a subprogram within RADAN is used to proportionally adjust the position of each radar scan according to the time stamp of the two nearest positions recorded with the GPS receiver. Position data were recorded with the GPS receiver at a time interval of one second.

The EM38-MK2 meter (Geonics Limited, Mississauga, Ontario) was used in a reconnaissance survey of Shale Hills Watershed.[1] The EM38-MK2 meter weighs about 2.8 kg (6.2 lbs) and requires only one person to operate. The EM38-MK2 meter consists of one transmitter coil and two receiver coils, and operates at a frequency of 14,500 Hz. The receiver coils are separated from the transmitter coil at distances of 100 and 50 cm. This configuration provides nominal penetration depths for the 100 and 50 cm coil spacings of 150 and 75 cm in the vertical dipole orientation (VDO) and 75 and 38 cm in the horizontal dipole orientation (HDO), respectively. Operating procedures for the EM38-MK2 meter are described by Geonics Limited (2008). The EM38-MK2 meter can provide simultaneous measurements of both quadrature-phase (conductivity) and in-phase (susceptibility) components within the two depth ranges.

A Trimble AgGPS114 L-band DGPS (differential GPS) antenna (Trimble, Sunnyvale, CA) was used with the EM38MK2-2 meter.[1] During surveying, EC_a and GPS measurements were automatically recorded in the Allegro CX field computer (Juniper Systems, Logan, Utah).[1] The Trackmaker38MK2-2 software programs

---

[1] Trade names are used for specific references and do not constitute endorsement.

developed by Geomar Software Inc. (Mississauga, Ontario) were used to record, store, and process EC_a and GPS data.[2] All EMI data are expressed as values of EC_a in milliSiemens/meter (mS/m).

To help summarize the results of the EMI survey, SURFER for Windows, version 9.0, developed by Golden Software, Inc. (Golden, CO), was used to construct the simulation shown in this report.[2] Grids of EC_a data were created using kriging methods with an octant search.

Calibration of GPR:
Ground-penetrating radar is a time scaled system. The system measures the time that it takes electromagnetic energy to travel from an antenna to an interface (e.g., bedrock, soil horizon, stratigraphic layer) and back. To convert the travel time into a depth scale, either the velocity of pulse propagation or the depth to a reflector must be known. The relationships among depth (D), two-way pulse travel time (T), and velocity of propagation (v) are described in equation [1] (after Daniels, 2004):

$$v = 2D/T \qquad [1]$$

The velocity of propagation is principally affected by the relative dielectric permittivity (E_r) of the profiled material(s) according to equation [2] (after Daniels, 2004):

$$E_r = (C/v)^2 \qquad [2]$$

Where C is the velocity of propagation in a vacuum (0.298 m/ns). Typically, velocity is expressed in meters per nanosecond (ns). In soils, the amount and physical state (temperature dependent) of water have the greatest effect on the E_r and v.

Based on the measured depth and the two-way pulse travel time to a known subsurface reflector (metal plate buried at 50 cm), the velocity of propagation and the relative dielectric permittivity through the upper part of a Rushtown (loamy-skeletal over fragmental, mixed, active, mesic Typic Dystrudepts) soil profile were estimated using equations [1] and [2]. At the time of these studies, soils were moist. In an area of Rushtown soil, the estimated E_r was 12.4. This permittivity results in an estimated v of 0.0846 m/ns.

Resolution:
Ground-penetrating radar radiates and receives electromagnetic energy in a complex 3D cone (Neal, 2004). Resolution is dependent on antenna frequency as well as the relative dielectric permittivity and velocity of signal propagation through the medium. Vertical resolution is dependent upon the wave length (λ) of the antenna. The λ is governed by the antenna frequency (f) and the velocity of propagation (v) according to the formula (after Neal, 2004):

$$\lambda = v/f \qquad [3]$$

In this study, an antenna with a center frequency of 400 MHz was used. The E_r of the soil material was 12.4 and v was 0.0846 m/ns. According to equation [3], the estimated λ is 0.21 m. Under ideal conditions, resolution is assumed to be equal to about third (λ /3) to one-half (λ /2) of the input wave length (Beres and Haeni, 1991). Based on these assumptions, the vertical resolution of the 400 MHz antenna at the Shale Hills Watershed would range from about 5 to 7 cm. Interfaces separated vertically by less than λ /3 λ /2 will be poorly resolved and obscured by constructive and destructive interference. In most situations, however, background noise, velocity and wave form variations limit resolution to one quarter of the input wave length (λ /4) (Lane et al., 2000).

Horizontal resolution depends on antenna frequency, depth to the reflecting surface, and the dielectric permittivity of the profiled material. The use of higher frequency (and shorter wave length) antennas will provide greater horizontal resolution. In general, a higher E_r (wetter soil materials) will result in a more focused

---

[2] Trade names are used for specific references and do not constitute endorsement.

radar beam and greater horizontal resolution. The equation for estimating the approximate size of the footprint area scanned beneath the radar is (after Neal, 2004):

$$A = \lambda/4 + D/\sqrt{E_r - 1} \qquad [4]$$

Where A is the radius of the footprint area, λ is wave length, D is the depth to the reflector, and E_r is the relative dielectric permittivity. Horizontal resolution will decrease as the footprint area expands with increasing soil depth. According to equation [4], fracture, cleavage planes, and other discontinuities will be more poorly imaged and positioned in the lower than in the upper parts of radar records.

The Shale Hills Watershed is incised into a shale ridge composed of the Rose Hill formation, Clinton Group of middle Silurian age. The Rose Hill formation consists of a sequence of thinly bedded, highly fractured, folded and faulted, olive and purplish shale with thin, intermixed beds of hematite sandstone and fossiliferous limestone. Observed cleavage planes in the Rose Hill formation are very thin (0.1 to 1.3 cm) and are below the resolution of the 400 MHz antenna. While the wave length of the 400 MHz is too large to resolve closely spaced cleavage planes in areas of Rose Hill formation, some larger fracture and cleavage planes filled with moisture will be detectable. The detection of fracture and bedding plane often depends on the thickness and the material filling the discontinuity. High-amplitude radar reflections have been associated with abrupt changes in water content that occur in filled joints, fractures, and structural planes (Lane et al., 2000; Buursink and Lane, 1999; Olhoeft, 1998; Grasmueck, 1996).

As bedding, cleavage and fracture planes become more vertically inclined, they reflect increasingly less energy back to the antenna and therefore provide poorer reflecting surfaces. Fractures and structural planes with dip-angles greater than about 45^o are affected by spatial aliasing distortion and are not accurately imaged with GPR (Buursink and Lane 1999; Ulriksen, 1982). Spatial aliasing restricts the dip-angles that are detectable with GPR (Lane et al., 2000). More vertically inclined interfaces reflect very little energy back towards the radar antenna. As a consequence, these reflectors often appear on radar records as low-amplitude diffractions whose alignment reflects the orientation of the steeply inclined fracture (Grasmueck et al., 2004).

Field Methods:

The Shale Hills Watershed is underlain by fractured rock. In this study, GPR is used to better understand and characterize preferential flow paths in soils over fractured bedrock, at scales of one to several meters. Two grid sites are located areas of Rushtown soils. The very deep, excessively drained Rushtown soils formed in colluvial deposits. Both Rushtown grid sites are located middle of concave swales that descend downwards along a south-facing slope in the Shale Hills Watershed. The dimensions of one Rushtown grid are 150 by 90 cm. A total of ten, 150-cm traverses were completed across this grid with a 400 MHz antenna. Traverse lines were orientated essentially orthogonal to the slope. The interval between successive traverse lines was 10 cm.

The second Rushtown grid site had overall dimensions of 12 by 15 ft. Plastic stakes have been inserted in the ground at the four grid corners and a rope grid-lattice has been fabricated for attachment to these stakes and overlaid across the grid area. The rope lines extend across the grid (parallel with X axis) and provide ground control. Each rope line is distance-graduated with distance marks affixed at intervals of 5 feet. A total of eleven, 15-ft traverses were completed across this grid with a 400 MHz antenna. Traverse lines were orientated essentially orthogonal to the slope. The interval between successive traverse lines was 13 inches.

The Weikert site is located along a plane, south-facing side slope. The shallow, well drained Weikert soils formed in material that weathered from interbedded gray and brown acid shale, siltstone, and fine-grained sandstone on gently sloping to very steep areas. Weikert is a member of the loamy-skeletal, mixed, active, mesic Lithic Dystrudepts family. The dimensions of the Weikert grid are 200 by 100 cm. A total of eleven, 200-cm traverses were completed across this grid with a 400 MHz antenna. Traverse lines were orientated essentially orthogonal to the slope. The interval between successive traverse lines was 10 cm.

Results:

Subsurface flow:

Many factors influence subsurface flow. Factors include soil, stratigraphic, and lithologic layering, complex macropore systems, and soil pipes caused by shrink-swell phenomena, animal borrows, and tree roots. In a research article that was submitted to Hydrological Processes (Zhang et al., 2010), results from GPR studies suggest that subsurface lateral flow dominates areas of the shallow Weikert soils and subsurface vertical flow dominates areas of the very deep Rushtown soils. Using simulated radar images generated by four conceptual flow models and GPR field records, these researchers found that, within the Shale Hills Watershed, subsurface lateral macropore flow dominated areas of Weikert soils, while vertical macropore and lateral matrix flows dominated areas of Rushtown soils.

Ground-penetrating radar surveys were conducted across three small grid sites to observe temporal differences in subsurface reflections associated with the flow of water through profiles of Rushtown and Weikert soils. Appendix 1 lists the radar file numbers associated with different traverses in these grid sites. Figure 1 shows pseudo-images of the radar records collected on the Weikert and Rushtown grid sites. With the 400 MHz antenna, the depth of observable reflections was deeper in Rushtown (about 2.25 m) than Weikert (about 1.5 m) soils. Both soils are characterized by multiple, closely-spaced, planar reflectors (Fig. 1). These reflectors, however, appear more continuous and less segmented in the Weikert pseudo-image (Fig. 1). This suggests that layering caused by soil horizons and stratigraphic or lithologic layers is relatively more continuous with less opportunities for vertical preferential flow paths beneath Weikert than Rushtown soils. These spatial patterns appear to corroborate the findings of Zhang et al. (2010) that subsurface lateral macropore flow dominated in areas of Weikert soils, while vertical macropore and lateral matrix flows dominated areas of Rushtown soils.

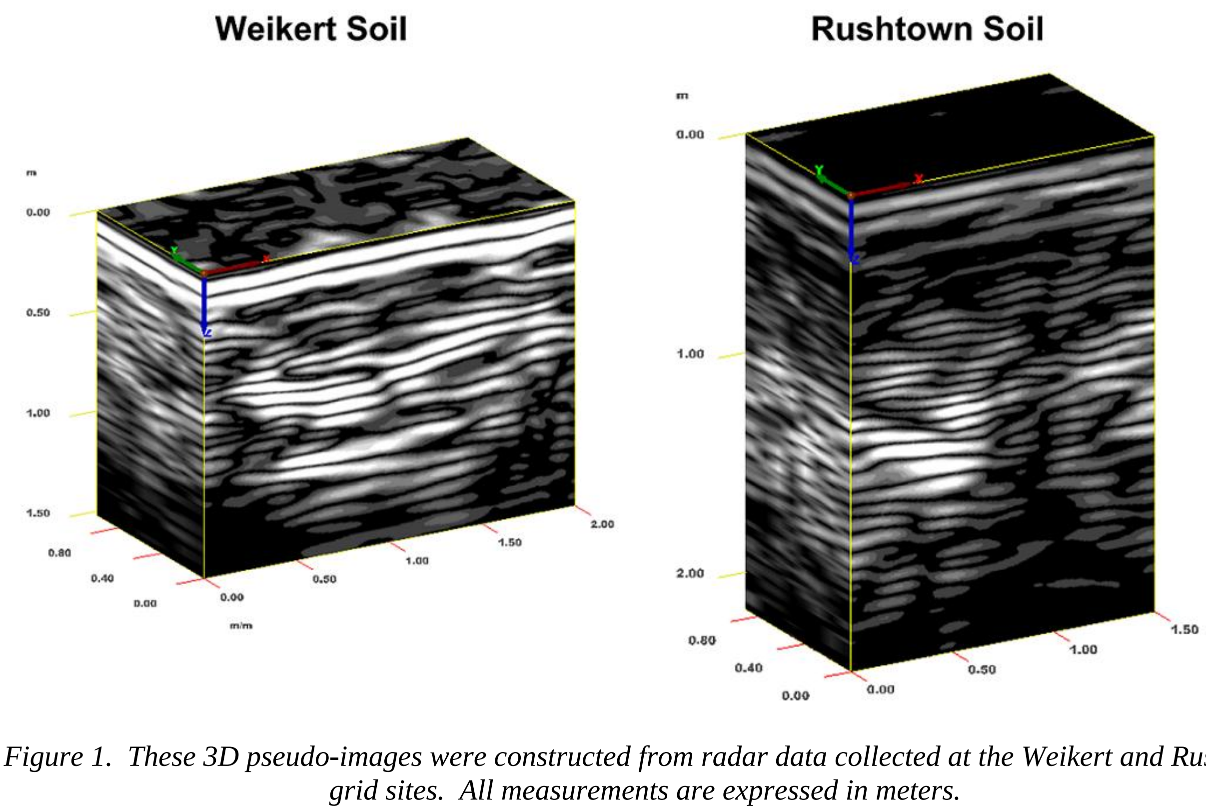

Figure 1. These 3D pseudo-images were constructed from radar data collected at the Weikert and Rushtown grid sites. All measurements are expressed in meters.

GPR-GPS:

Lin (2010) remarks on the present inability to adequately characterize subsurface soil heterogeneities and to bridge scales (e.g., point, watershed, global) in hydropedological investigations. Lin (2010) also calls attention to the significant gap that exists in hydropedological information at intermediate scales (e.g., watershed scales), because of the limitations of existing tools and techniques. The recent integration of GPR with GPS and the use of interactive interpretation software provide new approaches for characterization of soils at intermediate scales. These cutting-edge tools may help to overcome the existing *technological bottleneck* that is described by Lin (2010).

The SIR-3000 can be used with a suitable GPS receiver and serial data recorder (SDR) to georeference the radar data for display in imaging software such as Google Earth and geographic information systems (GIS). With this setup, each scan on a radar record is essentially georeferenced (position/time matched). GPR readings (scans) are not continuous, but are taken at set time intervals. In this study, the scanning rate was 64 scans/sec. With the Trimble ProXT GPS receiver, position data were recorded at a rate of one measurement/sec. In RADAN, the position of each radar scan is proportionally adjusted according to the time stamp of the two nearest positions recorded with the GPS receiver. As each scan of the radar is georeferenced, the integration of GPS with GPR results in incredibly large data sets.

Using the *Interactive Interpretation* module of RADAN, depths to the soil-bedrock interface were quickly, automatically, and reasonably accurately picked and outputted to a worksheet (X, Y, Z format; containing latitude, longitude, depths to contrasting interface, and other useful data). Using the *Interactive Interpretation* module, radar data can be easily exported into Microsoft Excel for documentation and statistical analysis, and into GIS for plotting and visualization.

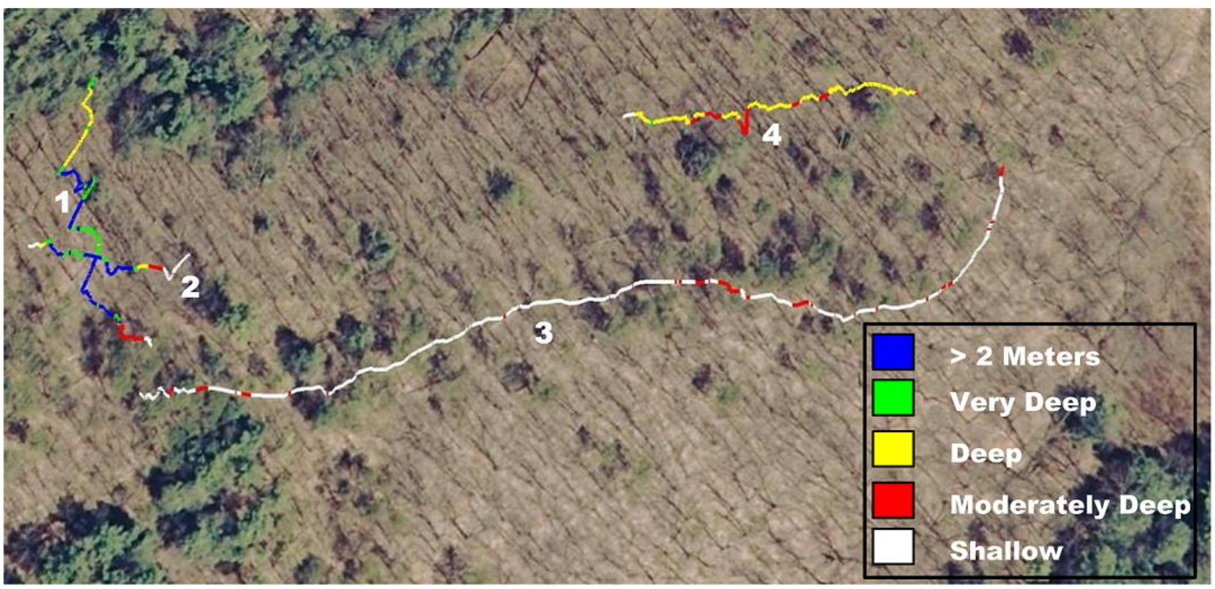

Figure 2. In this Google Earth image of the southern portion of the Shale Hills Watershed, the locations of georeferenced GPR traverse lines are shown. Colors indicate the depths to bedrock according to soil depth classes.

During this field study, four radar traverses were conducted along north facing slopes and the southern ridge-line perimeter to the Shale Hills Watershed (see Fig. 2). Steeper portions of the traversed areas are mapped as Berks-Weikert shaly silt loams, 15 to 25 percent slopes (BiD) and Berks-Weikert association, steep (BmF). Along lower-lying and less sloping drainage channel areas, soils are mapped as Ernest silt loam, 3 to 8 percent slopes (ErB). The well drained, moderately deep Berks soils form in materials weathered from acid shales on uplands. Berks soils are members of the loamy-skeletal, mixed, active, mesic Typic Dystrudepts taxonomic family. The very deep, moderately well and somewhat poorly drained Ernest soils form in colluvium derived from acid shale. Ernest soils are members of the fine-loamy, mixed, superactive, mesic Aquic Fragiudults taxonomic family. All of these soils are considered to have moderately potential for GPR (http://soils.usda.gov/survey/geography/maps/GPR/index.html).

Using the *Interactive 3D Module* of RADAN, depths to the soil-bedrock contact were quickly picked and recorded in a layer file. Figure 2 contains a Google Earth image of the area traversed with GPR within the Shale Hills Watershed (in Figure 2, different colors are used to represent the different soil depth classes). Traverse lines 1 and 2 were along the centerline and orthogonal to a major swale, respectively. Soils were principally very deep along these traverse lines. Traverse line 3 was along the watershed's southern perimeter trail. Soils were dominantly shallow and moderately deep along traverse line 3. Traverse line 4 cuts diagonally across a lower, north-facing side slope component. Here, soils are chiefly within the moderately deep to deep soil depth classes.

EMI Survey:

For the EMI survey of the Shale Hills Watershed, the EM38-MK2-2 meter was operated in the deeper-sensing, vertical dipole orientation (VDO). Apparent conductivity data were recorded for both the 50 and 100 cm intercoil spacings. The EM38-MK2-2 meter was operated in the continuous (measurements recorded at a rate of 1/sec) mode. Using the TrackmakerEM38MK2 program, both GPS and EC_a data were simultaneously recorded in an Allegro CX field computer.

While surveying, where possible, the EM38-MK2-2 meter was held about 5 cm (about 2 inch) above the ground surface. The meter was orientated with its long axes parallel to the direction of traverse. Steep slopes, under-brush, tree limbs, and fallen forest debris made walking difficult and caused the meter to vary in height. Where possible, traverses were conducted parallel with the slope contours. Multiple traverses were conducted across and along the center-line of swales. Terrain obstructions, satellite shading and multipath reception reduced the accuracy and reliability of GPS positioning on lower slopes, especially beneath the evergreen canopy along the lower reach of the stream. The EC_a data discussed in this report were not temperature corrected.

Table 1
Some Basic Statistics for the EMI Surveys
of the Shale Hills Watershed that was conducted with an EM38MK2-2 meter.

	100 cm	**50 cm**
Observations	9429	9429
Minimum	0.41	0.04
Maximum	34.31	39.73
25% Quartile	5.13	5.16
75% Quartile	7.44	8.09
Mean	6.44	7.60
Std. Deviation	2.32	4.16

Basic statistics for April 2010 survey are shown in Table 1. Anomalously high and negative EC_a values have been removed from the data set. These values were associated with metallic artifacts scattered across this research site and improper calibration.

This was the first survey that was completed with the newly developed EM38MK2-2 meter within the Shale Hills Watershed. Results from this survey are comparable with those previously collected with the EM38 meter during wetter, spring months. For measurements collected with the deeper-sensing (0 to 150 cm depth interval), 100 cm intercoil spacing, EC_a averaged only 6.4 mS/m and ranged from 0.4 to 34.3 mS/m. One half the measurements collected with this intercoil spacing had values of EC_a between about 5.1 and 7.4 mS/m. For measurements collected with the shallower-sensing (0 to 75 cm depth interval), 50 cm intercoil spacing, EC_a averaged 7.6 mS/m and ranged from 0.04 to 39.7 mS/m. One half the measurements made with this intercoil spacing had values of EC_a between about 5.2 and 8.1 mS/m.

Figure 3 is a two-dimensional plot of the EC_a data that were measured with the EM38MK2-2 meter in the deeper-sensing, 100-cm intercoil spacing. Dotted blue lines represent the locations of the stream channel and the center lines of major swales that extend upslope from this channel.

The Shale Hills Watershed is characterized by exceedingly low and relatively invariable EC_a. Spatially, lower EC_a is recorded on higher-lying, plane and convex back slopes (see Fig.3). These landscape components are dominated by the shallow Weikert soil and moderately deep Berks soils. Areas of higher EC_a are evident along the stream channel. Ernest and Blairton soils occur on this portion of the landscape. Compared with other soils recognized within this watershed, these soils have higher moisture contents and shallower depths to water table. The linear strip of higher EC_a evident along the northwestern boundary of the watershed represents recently buried utility cables which run beneath the trail leading to a weather and instrument station.

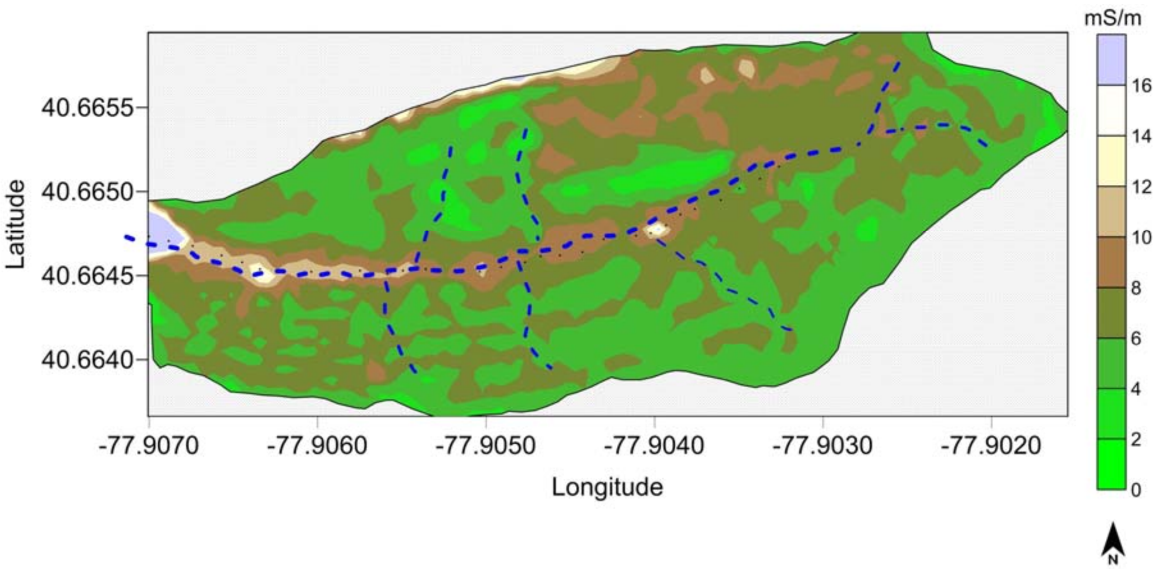

Figure 3. Plot of EC_a data collected in the Shale Hills Watershed with EM38MK2-2 meter with the deeper-sensing 100-cm intercoil spacing.

References:

Beres, M. and F.P. Haeni, 1991. Application of ground-penetrating-radar methods in hydrogeologic studies. *Ground Water* 29(3): 375-386.

Buursink, M.L., and J. W. Lane, 1999. Characterizing fractures in a bedrock outcrop using ground-penetrating radar at Mirror Lake, Grafton County, New Hampshire. 769-776 pp. IN: Morganwalp, D.W., and Buxton, H.T. (eds.), U.S. Geological Survey Toxic Substances Hydrology Program--Proceedings of the Technical Meeting, Charleston, South Carolina, March 8-12, 1999--Volume 3 of 3--Subsurface Contamination from Point Sources: U.S. Geological Survey Water-Resources Investigations Report 99-4018C.

Daniels, D.J., 2004. Ground Penetrating Radar; 2nd Edition. The Institute of Electrical Engineers, London, United Kingdom.

Geonics Limited, 2008. EM38-MK2 ground conductivity meter operating manual. Geonics Limited, Mississauga, Ontario.

Grasmueck, M., 1996, 3-D ground-penetrating radar applied to fracture imaging in gneiss: *Geophysics*, v. 61, no. 4, p. 1050-1064.

Grasmueck, M., R. Weger, and H. Horstmeyer, 2004. Three-dimensional ground-penetrating radar imaging of sedimentary structures, fractures, and archaeological features at submeter resolution. *Geology* 32(11): 933-936.

Jol, H., 2009. Ground Penetrating Radar: Theory and Applications. Elsevier Science, Amsterdam, The Netherlands.

Lane Jr., J. W., M. L. Buursink, F. P. Haeni, and R. J. Versteeg, 2000. Evaluation of ground-penetrating radar to detect free-phase hydrocarbons in fractured rocks – results of numerical modeling and physical experiments. *Ground Water* 38(6): 929-938.

Lin, H., 2010. Earth's Critical Zone and hydropedology: concepts, characteristics, and advances. *Hydrology and Earth System Sciences* 14: 25-45.

Neal, A., 2004. Ground-penetrating radar and its use in sedimentology: principles, problems and progress. *Earth-Science Reviews* 66: 261-330.

Olhoeft, G., 1998. Electrical, magnetic, and geometric properties that determine ground penetrating radar performance. 177-182 pp. IN: Plumb, R. G. (ed.) Proceedings of the Seventh International Conference on Ground-Penetrating Radar. May 27 to 30, 1998, Lawrence, Kansas. Radar Systems and Remote Sensing Laboratory, University of Kansas.

Zhang, J., H. Lin, and J. Doolittle, 2010. Hillslope subsurface flow revealed by time-lapsed ground penetrating radar and real-time soil moisture monitoring. *Hydrological Processes* (paper submitted).

Ulriksen, C.P.F., 1982. Application of impulse radar to civil engineering. Ph.D. dissertation. Lund University of Technology. Lund, Sweden.

Appendix 1: GPR File Numbers associated with different radar traverses and study sites.

File 1	400 MHz antenna – plate at 50 cm.
File 2	900 MHz antenna – plate at 50 cm.
Files 5-15	Weikert Grid – 400MHz antenna; 62 scans/sec, scale is metric.
File 16	400 MHZ antenna– plate at 1.75 ft.
Files 17 – 28	Permanent Grid -400 MHz antenna; 62 scans/sec; scale in feet; first survey.
Files 29 – 40	Permanent Grid -400 MHz antenna; 62 scans/sec; scale in feet; second survey.
Files 41 – 51	Rushtown Site 2 (150 x 90 x 10 (spacing) cm grid; 400 MHz antenna; metric.
Files 52 – 53	Opened Auger Hole in Rushtown Site 2.
Files 54+	GPR – GPS of north-facing slopes with 400 MHz antenna.